Mole Quantity of RPE65 and Its Productivity in the Generation of 11-*cis*-Retinal from Retinyl Esters in the Living Mouse Eye†

Arkady L. Lyubarsky,‡ Andrey B. Savchenko,‡ Sarah B. Morocco,‡ Lauren L. Daniele,‡ T. Michael Redmond,§ and Edward N. Pugh, Jr.*,‡

F. M. Kirby Center for Molecular Ophthalmology, Department of Ophthalmology, School of Medicine, University of Pennsylvania, 422 Curie Boulevard, Philadelphia, Pennsylvania 19104-6069, and Laboratory of Retinal Cell and Molecular Biology, National Eye Institute, National Institutes of Health, Bethesda, Maryland 20892

Received March 23, 2005; Revised Manuscript Received May 19, 2005

ABSTRACT: RPE65, a protein expressed in cells of the retinal pigment epithelium of the eye, is essential for the synthesis by isomerohydrolase of 11-*cis*-retinal, the chromophore of rod and cone opsins. Recent work has established that RPE65 is a retinyl ester binding protein, and as all-*trans*-retinyl esters are the substrate for isomerohydrolase activity, the hypothesis has emerged that RPE65 serves to deliver substrate to this enzyme or complex. We bred mice with five distinct combinations of the RPE65 Leu450/Met450 variants (Leu/Leu, Met/Met, Leu/Met, Leu/−, and Met/−), measured in mice of each genotype the mole quantity of RPE65 per eye, and measured the initial rate of rhodopsin regeneration after a nearly complete bleach of rhodopsin to estimate the maximum rate of 11-*cis*-retinal synthesis in vivo. The quantity of RPE65 per eye ranged from 5.7 pmol (Balb/c) to 0.32 pmol (C57BL/6N × *Rpe65*$^{-/-}$); the initial rate of rhodopsin regeneration was a Michaelis function of RPE65, where V_{max} = 18 pmol/min per eye and K_m = 1.7 pmol, and not dependent on the Leu450/Met450 variant. At RPE65 levels well below the K_m, the rate of production of 11-*cis*-retinal per RPE65 molecule was ∼10 min^{-1}. Thus, the results imply that as a chaperone each RPE65 molecule can deliver retinyl ester to the isomerohydrolase at a rate of 10 molecules/min; should RPE65 itself be identified as the isomerase, each copy must be able to produce at least 10 molecules of 11-*cis*-retinal per minute.

The visual retinoid cycle comprises a series of enzymes and retinoid-binding chaperones or retinoid binding proteins. These proteins govern the synthesis of the visual chromophore, 11-*cis*-retinal,[1] deliver the chromophore to opsins in rods and cones, and remove and recycle all-*trans*-retinal, generated stoichiometrically after each photoisomerized chromophore inititates phototransduction and is subsequently hydrolyzed from the opsin (reviewed in refs *1* and *2*). An essential enzymatic activity of the cycle is the isomerohydrolase (*3*), which produces 11-*cis*-retinoid in the retinal pigment epithelial (RPE) cells situated in the eye immediately behind the rod and cone photoreceptor outer segments. While the protein or protein complex underlying isomerohydrolase activity remains to be identified, key features of its activity have been established. First, the substrate for the isomerohydrolase is all-*trans*-retinyl ester (*4*, *5*); second, the product of the isomerohydrolase activity is 11-*cis*-retinol (*6*), which must be subsequently oxidized to 11-*cis*-retinal by a stereospecific dehydrogenase (*7*).

One essential protein of the retinoid cycle is RPE65, an ∼65 kDa protein expressed in RPE cells (*8*−*10*). Mutations in RPE65 give rise to Leber's congenital amaurosis, an early onset, debilitating retinal dystrophy (*11*, *12*). Mice null for RPE65 (*Rpe65*$^{-/-}$) have vastly reduced visual sensitivity, with no measurable rhodopsin, leading to the conclusion that in the absence of RPE65, 11-*cis*-retinal cannot be synthesized (*13*). Indeed, the residual visual sensitivity of *Rpe65*$^{-/-}$ mice is due to trace amounts of an alternative functional chromophore, 9-*cis*-retinal, likely created in a synthetic pathway distinct from that involved in 11-*cis*-retinal synthesis (*14*). The biochemical role of RPE65 in the visual retinoid cycle has been elucidated by experiments that revealed it be a high-affinity retinyl ester binding protein (*15*, *16*). In the context of the essential role of retinyl esters in 11-*cis*-retinal biosynthesis by isomerohydrolase activity (*4*, *5*, *17*), it has been concluded that RPE65's primary role in the visual retinoid cycle is to deliver all-*trans*-retinyl ester to this enzyme or enzyme complex in the smooth endoplasmic reticulum of the RPE cell (*15*, *16*). However, the hypothesis that RPE65 is itself the isomerase is a matter of active debate (*18*).

The regeneration of rhodopsin in all mammalian species that have been adequately characterized is rate-limited; thus, after the exposure of the eye to a light that bleaches most of the pigment, the regeneration of rhodopsin initially proceeds as a linear function of time, the maximum rate that can be achieved in a given eye (*2*). The maximal rate varies substantially across species; for example, it is ∼4.5-fold higher in the human eye (9% rhodopsin min^{-1}) than in the

† Supported by NIH Grant EY02660 and the Research to Prevent Blindness Foundation.

* To whom correspondence should be addressed. Phone: (215) 898-2403. Fax: (215) 573-7155. E-mail: pugh@mail.med.upenn.edu.

‡ University of Pennsylvania.

§ National Institutes of Health.

[1] Abbreviations: 11-*cis*-retinal, 11-*cis*-retinaldehyde; all-*trans*-retinal, all-*trans*-retinaldehyde; RPE, retinal pigment epithelium; SER, smooth endoplasmic reticulum; CTACl, cetyltrimethylammonium chloride; GAPDH, glyceraldehyde phosphate dehydrogenase; AP, alkaline phosphatase; EtOH, ethanol; SDS−PAGE, sodium dodecyl sulfate−polyacrylamide gel electrophoresis.

10.1021/bi0505363 CCC: $30.25
Published on Web 06/25/2005

murine strains with the highest measured rates ($\sim$2% min^{-1}) (*2*). In mice, the maximal rate of rhodopsin regeneration is strain-dependent, being approximately 4-fold higher in Balb/c and 129Sv mice, which express the Leu450 variant of RPE65, than in C57BL/6J and B6;129S(N2) mice, which express the Met450 variant (*19*). Because the level of RPE65 expression is also strain-dependent (*19*), we undertook to determine the mole quantity of RPE65 in several lines of mice with distinct levels of expression of the protein, to determine the initial rate of regeneration in each line, and to assess the dependence of the regeneration rate on RPE65 quantity and on the Leu450/Met450 variant.

EXPERIMENTAL PROCEDURES

Animal Husbandry. All animal procedures were performed in adherence with protocols approved by the Institutional Animal Care and Use Committee of the University of Pennsylvania, in accordance with the regulations of the National Institutes of Health. Six-week-old mice were obtained from Charles River (Wilmington, MA). Animals were reared in a 12 h (from 8:00 a.m. to 8:00 p.m., 2.5 lux) light cycle and dark-adapted overnight before the experiments.

Breeding and Genotyping. Rpe65$^{-/-}$ were produced as described previously (*13*), and were crossbred with C57BL/6N or Balb/c mice. Tailsnip DNA was prepared with the Puregen kit (Gentra, Minneapolis, MN). The null allele for *Rpe65* was probed with the following primers: forward, 5′-GGG AAC TTC CTG ACT AGG GGA GG-3′; and reverse, 5′-CCC AAT AGT CTA GTA ATC ACA GAT G-3′. The WT allele was probed with the primers: forward, 5′-GAT GTG GGC CAG GGC TCT TTG AA-3′; reverse, same that was used for the null allele. *Rpe65* cDNA analysis was used to distinguish the Leu450 and Met450 variants of the protein, as described below (*Rpe65 Sequence Analysis and Real Time PCR*).

Rhodopsin Bleaching and Regeneration in Vivo. Before the experiment commenced, the pupils of mice dark-adapted overnight were dilated by application of a cocktail containing 2% atropine and 1% phenylephrine. Approximately 10−12 min after the cocktail application, when the pupils were fully dilated (*20*), the mouse was placed into a clear perforated plastic jar which, in turn, was placed onto the bottom of a ventilated box lined with aluminum foil with two fluorescent tubes (SLI, El Paso, TX) on the box's ceiling: 7 W tubes were used for albino mice, and 20 W for pigmented mice, to provide approximately equivalent retinal illumination. Mice were illuminated for 10 min, and allowed to regenerate rhodopsin in complete darkness for predetermined intervals of time. At all times, the animals were awake, and no anesthesia was used. This protocol closely followed that of ref *19*, with the exception of the use of illumination levels that equated the retinal light loads for albino and pigmented mice (*20*).

Rhodopsin Measurement. The mole quantity of rhodopsin was measured in each line of mice investigated with the extraction method of Saari and colleagues (*21*), and bleaching difference spectroscopy, assuming a molar extinction coefficient of 42 000 L mol^{-1} cm^{-1} at 500 nm. For measuring the fraction of rhodopsin regenerated after a bleaching exposure, we employed the method described in ref *20*. In this method, immediately after an animal is sacrificed, its retinas are harvested through slits in the corneas and solublized in deionized water. The solute is then divided into two aliquots and incubated at 37 °C for 20 min: one aliquot is untreated, and to the other is added 11-*cis*-retinal to fully regenerate rhodopsin. The fraction rhodopsin present in the eyes at the time of sacrifice is obtained from the ratio of rhodopsin in the two samples.

Protein Quantification. One goal of this work was to determine the absolute quantity of RPE65 in each of five lines of mice. To achieve this goal, we needed to be sure that we extracted all of the protein from the eye. The most complete solubilization of the entire protein content of the eyecup (eye with lens and cornea removed) was achieved when Laemmli sample buffer was used to effect the solubilization, so the sample was ready for SDS−PAGE analysis in one step. As standard protein assays such as the Bradford or Lowry methods are incompatible with the use of Laemmli buffer because of the high concentrations of SDS and DTT, we developed an alternative method in which known amounts of reference proteins GAPDH or BSA were added to lanes of SDS−PAGE gels and GelBlue (Pierce, Rockford, IL) coomassie stain was applied, followed by quantitative densitometric analysis. With this method, we obtained an estimate of the total protein of 2.6 $\pm$ 0.4 mg per eyecup (mean $\pm$ standard error of the mean).

Antibodies. For immunoblotting, polyclonal rabbit antibodies raised against amino acids 150−164 of human/bovine RPE65 (*22*) were used at a dilution of 1:2000, and against β-actin (ab8227 from Abcam, Inc., Cambridge, MA) at 1:5000.

Recombinant RPE65. A bovine RPE65 cDNA template was amplified using oligonucleotides supplied with the Rapid Translation System (RTS) linear template generation set, His-tag (Roche Applied Science). The resultant PCR product with T7 regulatory elements and a C-terminal His tag was subcloned into the pCR4TOPO (Invitrogen) vector. The derived plasmid was purified and used as a template for an in vitro transcription and translation system (RTS 500 HY kit, Roche Applied Science). Expressed protein was recovered from the insoluble pellet after incubation for 23 h by solubilization in 6 M guanidine hydrochloride. Solubilized polyHis-tagged RPE65 protein was then captured on magnetic beads by immobilized metal affinity chromatography by incubating 1 mL of the solubilized protein with 8 mg of Talon Dynabeads (Dynal, Brown Deer, WI) at 4 °C with rocking for 1 h. The tube was then placed in a magnetic stand, and the magnetic beads were recovered. The supernatant was drawn off, and the tube was then removed from the stand. The magnetic beads were washed three times by resuspension with 700 μL of 50 mM phosphate buffer containing 300 mM NaCl and 0.01% Tween, capturing the beads between each wash by placing in the magnetic stand. After the last wash, the drained captured beads were resuspended in 200 μL of 50 mM phosphate buffer containing 300 mM NaCl and 0.01% Tween. To release the rRPE65, the beads were sedimented by centrifugation and resuspended in Laemmli buffer, and the concentration was determined as described above (Protein Quantification).

Immunoblotting. Mice whose eyes were used for protein quantification underwent the identical illumination regimen as used in assessment of rhodopsin regeneration (see above). The mice were sacrificed after 20 min of recovery in

darkness, and the eyes were enucleated; the lens was removed, and one or two eyecups were homogenized for 30−40 s in 0.5 mL of iced Laemmli sample buffer (Bio-Rad, Hercules, CA) to which a protease inhibitor cocktail [protease inhibitors aprotinin and leupeptin (10 μg/mL)] had been added. The sample was sonified, heated in a boiling water bath for 5 min, and clarified by centrifugation at 7000*g* for 3 min. For immunoblotting, proteins separated by SDS−PAGE (6−50 μg/lane) were transferred onto Immobilon P membrane (Millipore, Billerica, MA) according to the manufacturer's instructions. Unless otherwise specified, the membranes were probed with primary antibodies for 20 h, washed, and probed with AP-conjugated anti-rabbit secondary antibodies (Bio-Rad) in a 1:10000 dilution. Immunoreactivity was visualized with ECF substrate (Amersham-Pharmacia, Piscataway, NJ) and recorded by scanning with a Storm 860 Phosphorimager (Molecular Dynamics, Sunnyvale, CA). The recorded immunoblot signals were subsequently analyzed with ImageQuant software (Molecular Dynamics). Briefly, small rectangular regions was drawn circumscribing each blot, and the signal (with the local average background subtracted) was recorded. The data were subsequently processed with spreadsheet statistical analysis.

To determine the absolute (mole) quantity of RPE65 in immunoblots, known quantities of recombinant bovine RPE65 (rRPE65) fused with a six-His tag (*22*) were loaded on gels as standards for comparison with signals from eye extracts. Absolute quantification of RPE65 was only used for Balb/c eyes. For the other lines of mice, a relative quantification procedure was employed in which eye extract from a population of Balb/c eyes served as a standard against which the relative quantities of RPE65 in the other lines were gauged.

Rpe65 Sequence Analysis and Real Time PCR. Total RNA was prepared from whole eyes using the RNeasy kit (Qiagen, Valencia, CA). The RNase-free DNase kit (Qiagen) was used to digest the remaining genomic DNA, and 500−1000 ng of total RNA was then reverse-transcribed with the Reverse Transcription Reagents kit (Applied Biosystems) using oligodT primers. To determine the sequence of *Rpe65*, total RNA was reverse-transcribed, and a 400 bp fragment containing the Leu450/Met450 codon was amplified using the following primer pair: forward, 5′-GTC ACA CTG CCC CAT ACA ACT-3′; reverse, 5′-CAG CCC TGG CAA TTT CAC TCA A3′. PCR products were purified with the QIAquick kit (Qiagen) and sequenced. To determine the amount of the Leu450/Met450 variant, real time PCR was performed with Assays On Demand in an ABI 7000 thermocycler (Applied Biosystems, Foster City, CA); 10−50 ng of total reverse-transcribed RNA per well was used, and the cDNA products were sequenced. The quantity of *Rpe65* mRNA was determined relative to the amount of β-actin mRNA, following the manufacturer's guide, from the cDNA product. We thus determined the quantity of *Rpe65* mRNA in each strain, relative to the quantity of *Rpe65* mRNA in a reference sample derived from the eyes of three Balb/c mice.

Quantification of the Efficiency of RPE65 Protein Synthesis. To quantify the efficiency of RPE65 protein synthesis relative to the amount of message in a line of mice, we measured a "protein-to-message ratio". The quantity of RPE65 protein in a strain relative to that in the standard line, Balb/c, was expressed as

$$\text{Rpe65 protein relative to standard} = \frac{\dfrac{\text{RPE65}}{\beta\text{-actin}}}{\dfrac{\text{RPE65 in standard}}{\beta\text{-actin in standard}}} \quad (1a)$$

while the quantity of *Rpe65* message relative to that in the standard line was expressed as

$$\textit{Rpe65}\text{ message relative to standard} = \frac{\dfrac{\textit{Rpe}65\text{ mRNA}}{\beta\text{-actin mRNA}}}{\dfrac{\textit{Rpe}65\text{ mRNA in standard}}{\beta\text{-actin mRNA in standard}}} \quad (1b)$$

Finally, the protein-to-message ratio (PMR) was defined as the ratio of eq 1a to eq 1b:

$$\text{PMR} = \frac{\text{RPE65 protein relative to standard}}{\textit{Rpe65}\text{ mRNA relative to standard}} \quad (1c)$$

The numerators and denominator of eq 1a were determined with the protein assays described above, while the components of eq 1b were determined from the real time PCR analysis of mRNA. Expressions 1a and 1b might seem unduly complicated at first examination, but in fact are readily implemented with standard gel scanning software, and serve in effect as control measures in quantifying blot signals, alleviating various concerns. Thus, both the numerator and denominator in eq 1a are readily determined from the respective immunoblots, and employing the ratios of RPE65 blot signals to the β-actin signals in the corresponding lanes automatically adjusts for a variety of factors that affect the absolute magnitudes of signals and their variation between gels. Similar considerations apply to the numerator and denominator in eq 1b, employed to quantify relative message levels of *Rpe65* and β-actin. The linear behavior of the blot signals over the domain of protein loads used is the basis of the method.

RESULTS

Masking Occurs in the Immunoblotting of RPE65. Absolute quantification of the mass of a protein in a tissue by immunoblotting rests on comparison of signals generated from an extract of the tissue with known amounts of pure protein. An issue fundamental to the validity of quantitative immunoblotting is whether other proteins present in the tissue extract interfere with the interaction between the detecting antibody and the target protein. Figure 1 presents the results of an experiment that addresses this issue. Incrementally increasing amounts of rRPE65 alone, or combined with a fixed quantity (9 μg) of protein extract from the eye of an *Rpe65*$^{-/-}$ mouse, were loaded on the same gel and immunoblotted. On the basis of the comparable eye size and retinal morphology (*13*), the extract from the *Rpe65*$^{-/-}$ mouse can be expected to have an overall protein content and composition close to those of other mice, with the exception of the absence of RPE65. Comparison of the signals in the lanes with and without extract reveals a large reduction in the

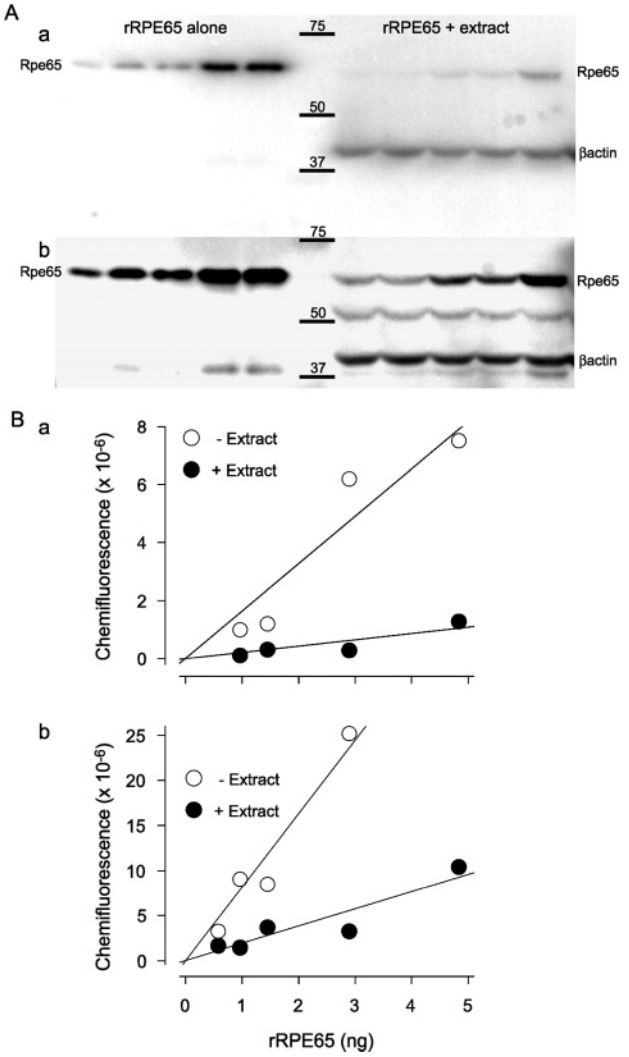

FIGURE 1: Masking of RPE65 in immunoblots by irrelevant protein components from the eye. (A) Immunoblot of five levels of recombinant RPE65 loaded on the gel alone (rRPE65 alone) or in combination with 9.2 μg of extract per lane from *Rpe65*$^{-/-}$ mice (rRPE65 + extract). The transfer membrane was probed with a combination of primary antibodies against RPE65 and against β-actin; the latter was used as a control for the extract load. The chemifluorescence signal is shown after incubation for 1 h with the antibodies at room temperature (a) and after 16 h at 4 °C (b). (B) Quantification of the immunoblots from panel A. Subpanels a and b correspond to the immunoblot images in panel A. Regression lines forced to pass through the origin were fitted to each set of data by least squares: in subpanel a, the slope of the line through the RPE65 blot signals of lanes with extract is 13% of that of the line through the signals of lanes without extract; in subpanel b, the slope of the line fitted to the RPE65 signals of lanes with extract is 24% of that of the line through the data of lanes with no extract. (The signals from the lanes with the highest rRPE65 loads were outside the linear range, and omitted from the regression analysis.)

extent of immunostaining for rRPE65, even for this relatively low protein load (Figure 1A, panel a). Incubating the transfer membrane for an additional 16 h with primary antibodies resulted in an increase in the RPE65 blot signal intensities (Figure 1A, panel b) in lanes with and without added extract, but relatively severe signal reduction persisted in the lanes to which extract from the eyes of *Rpe65*$^{-/-}$ mice was added. Prolonged incubation with the primary antibodies also resulted in the appearance of a band at ~52−55 kDa. As the intensity of this band did not vary with the quantity of rRPE65 (Figure 1A, panel b), and the band was further shown in control experiments with the extract of *Rpe65*$^{-/-}$ eyes to be generated by the interaction of the RPE65 antibody with a distinct protein, it was disregarded in the quantification of RPE65.

To quantify the masking effect, we compared the intensities of blots generated with varied amounts of rRPE65, loaded in the presence or absence of protein extract from the eye of the *Rpe65*$^{-/-}$ mouse (Figure 1B). The chemifluorescent signal intensities are described well in terms of a linear dependence of the signal on the mass of rRPE65 loaded into a lane. We quantified the masking effect ME of a particular level of protein extract in terms of the ratio of the slopes derived from blots in lanes with and without added extract. For the results in Figure 1B, ME = 0.13 for a 1 h and ME = 0.23 for a 16 h incubation with the primary antibodies. In additional experiments in which overnight incubation with the primary antibody was employed, ME was found to range from 0.2 to 0.5. We conclude that a relatively small amount of protein extract from the target tissue, but lacking the target protein RPE65, weakens the interaction of the antibody with RPE65 by 2−7-fold.

Absolute Quantification of RPE65 in Balb/c Mice. The overall strategy for quantifying RPE65 in the five lines of mice was to quantify the level absolutely in Balb/c mice, and then use eye extract from this line as a reference standard for relative quantification in the other lines. Balb/c mice were selected for the reference standard since previous work (*19*) indicated this strain to have the highest level of RPE65 expression. To obviate the masking artifact (Figure 1), immunoblot signals of Balb/c eye extract were compared with signals from two or more levels of recombinant protein, rRPE65, to which was added extract from eyes of *Rpe65*$^{-/-}$ mice at a level of protein matching that of the Balb/c reference sample (Supporting Information). From such experiments, we estimated the total mass of RPE65 per Balb/c eye to be 0.35 ± 0.02 μg. Assuming a molecular weight for of 61 000 (*9*, *23*), the amount of RPE65 per Balb/c eye is thus 5.7 ± 0.04 pmol.

Quantification of RPE65 in Lines of Mice Other than Balb/c. The amount of RPE65 in the eyes of another "target" line of mice relative to that in Balb/c eyes was determined from immunoblots in which several levels of extract from the target line and several from the reference sample were loaded onto the gels. To do this, we used a ratiometric approach (Methods, eq 1a), averaging the ratios of RPE65 and β-actin signals in each lane. Results of a typical experiment for one particular line of mice are illustrated in Figure 2; in this instance for the target line, Balb/c × *Rpe65*$^{-/-}$, the average immunoblot ratio is 0.11 ± 0.04 (mean ± standard deviation), while for the reference line, Balb/c, the ratio is 1.10 ± 0.06; the final estimate of the ratio of RPE65 in the target line relative to RPE65 in Balb/c (eq 1a) is 0.10.

Table 1 presents the results of applying the same analysis to immunoblots of eye extracts from the five murine lines investigated here. Balb/c mice, with 5.7 pmol/eye, have more than 4 times more RPE65 than any other line, and have 13-fold more RPE65 than C57BL/6N mice, and 18-fold more than the line with the lowest expression level, C57BL6 × *Rpe65*$^{-/-}$. The ratio of RPE65 to rhodopsin is ~1:100 in the Balb/c eye, and lower accordingly in the other mouse lines (Table 1).

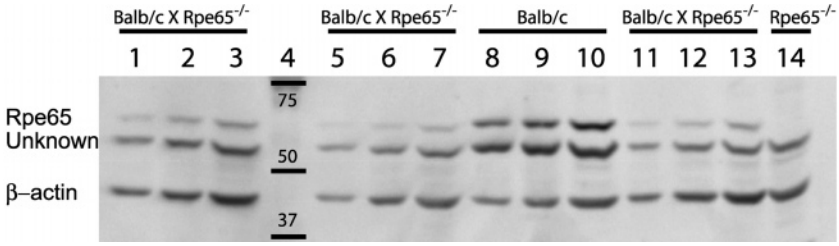

FIGURE 2: Immunoblot results from an experiment used to determine the amount of RPE65 in the eyes of Balb/c × *Rpe65*$^{-/-}$ mice (F1 cross) relative to that in the eyes of Balb/c mice, which served as the standard. Protein extract from the eyes of three different Balb/c × *Rpe65*$^{-/-}$ mice (lanes 1−3, 5−7, and 11−13) and from the standard Balb/c extract (lanes 8−10; cf. Figure 2) were loaded on the gel; extract from an *Rpe65*$^{-/-}$ mouse eye was loaded into lane 14 as a control. The amount of protein loaded was as follows: lanes 1−3, 11, 22, and 44 μg, respectively; lanes 5−7, 12, 24, and 48 μg, respectively; lanes 8−10, 6.75, 12.5, and 25 μg, respectively; lanes 11−13, 12.5, 25, and 50 μg, respectively; and lane 14, 36 μg. Lane 4 contained the molecular size markers.

Table 1: Quantitative Features of Rpe65 Message and Protein and Rhodopsin Quantity and Regeneration Rate in Various Mouse Lines[a]

strain or line	RPE65 status at AA450	*Rpe65* message per eye (referenced to BALB/c standard)	RPE65 protein (pmol/eye)	RPE65 protein/message (referenced to BALB/c standard)	rhodopsin (pmol/eye)	initial rate of rhodopsin regeneration (% min^{-1})
BALB/c	Leu/Leu	1	5.7 ± 1.2 (3)	1	590 ± 60 (4)	2.20 ± 0.48
C57BL6N × BALB/c	Leu/Met	0.96 ± 0.09 (2)	1.22 ± 0.26 (2)	0.21 ± 0.04	625 ± 51 (4)	1.17 ± 0.27
C57BL/6N	Met/Met	0.73 ± 0.11 (2)	0.42 ± 0.20 (2)	0.10 ± 0.05	630 ± 46 (4)	0.66 ± 0.13
BALB/c × *Rpe65*$^{-/-}$	Leu/−	0.60 ± 0.09 (2)	0.64 ± 0.28 (2)	0.18 ± 0.09	700 ± 26 (4)	1.0 ± 0.35
C57BL6 × *Rpe65*$^{-/-}$	Met/−	0.43 ± 0.03 (2)	0.32 ± 0.16 (2)	0.14 ± 0.07	660 ± 56 (4)	0.36 ± 0.16

[a] For each of the strains or lines listed in column 1, the table entries give the quantities (mean ± standard deviation) identified in the top row. For RPE65 protein (column 4), the results for Balb/c were obtained by absolute, quantitative analysis of immunoblots (Supporting Information); the mole quantities in the subsequent rows were obtained by multiplying the amount of RPE65 in each line of mice relative to Balb/c (eq 1a; cf. Figure 2) by the absolute amount determined for Balb/c mice. The numbers in parentheses give the numbers of animals from which the measurements were made; in most instances, independent measurements were made on each eye. (For error estimates of the rates of rhodopsin regeneration, see Figure 4.) A one-way analysis of variance was used to test the hypothesis that rhodopsin (column 6) varied between the lines; as there was no reliable effect, it was concluded that the amount of rhodopsin per eye was independent of the line, and the grand average value of 640 pmol/eye was used for calculations in Figure 5B.

Determination of the RPE65 Protein:Message Ratio. Previous work (*19*) has suggested that the level of *Rpe65* mRNA varies between murine strains to a much lesser degree than the level of RPE65 protein, leading to the hypothesis that the amino acid variant of RPE65 at position 450 (Leu450 vs Met450) may affect the protein's translation and/or stability. We measured a protein-to-message ratio, PMR, scaled relative to the ratio in Balb/c mice (Table 1, column 5; Experimental Procedures, eq 1c).

Kinetics of Rhodopsin Regeneration in Mice with Different Levels of RPE65. The variation among the five lines of mice in the expression of RPE65 protein provides a basis for examining the dependence of 11-*cis*-retinal production on RPE65 in vivo. We first measured the complete time course of rhodopsin regeneration in C57BL/6N and Balb/c mice after a short light exposure that bleached nearly all the rhodopsin, and compared our results with previously published data (Figure 3A). The time course of rhodopsin regeneration in both strains of mice is described well by a previously described model (Figure 3A, solid lines) (*2*). The predicted time course of regeneration is formally equivalent to that generated by the rate expression of Michaelis−Menten kinetics, expressible in terms of two parameters: V_{max}, a maximal velocity, and K_m, the fractional concentration of opsin at which regeneration velocity is half-maximal. The predicted initial rate of regeneration after a complete bleach is $V_{max}/(1 + K_m)$, since the fractional quantity of opsin cannot exceed unity. Because of the practical importance of the initial rate as an empirically measurable quantity, it is useful to identify it by a specific symbol; thus, $\nu = V_{max}/(1 + K_m)$. For Balb/c mice, $K_m = 0.2$ and $\nu = 0.024$ min^{-1}, while for C57BL/6 mice, $K_m = 0.2$ and $\nu = 0.0058$ min^{-1}.

After a strong bleach, rhodopsin regenerates over much of its time course as a linear function of time. As this rate-limited behavior is clearly exhibited by regeneration in both Balb/c and C57BL/6 strains (Figure 4A), whose RPE65 levels are near or at the extremes of several lines (Table 1), and as our interest was in understanding the dependence of the rate-limited phase of regeneration on the quantity of RPE65, in the three remaining strains we focused exclusively on this phase. At early times after a nearly complete bleaching exposure, rhodopsin regeneration in all five lines of mice exhibits a linear, rate-limited phase, whose rate was readily extracted with least-squares regression analysis (Figures 3B and 6C and Table 1).

Dependence of the Initial Rate of Regeneration on the RPE65 Level. Having estimated the mole quantity of RPE65 and the initial rate ν of rhodopsin regeneration in the five lines of mice, we analyzed the relationship between these two quantities, and found it to be described well by a hyperbolic saturation function (Figure 4A)

$$\nu = \nu_{max}\frac{\text{Rpe65}}{\text{Rpe65} + k_m} \qquad (2)$$

where $\nu_{max} = 2.75\%$ min^{-1} and $k_m = 1.52$ pmol/eye.

Productivity of RPE65 in 11-cis-Retinal Synthesis. For the three lines of mice with the smallest quantities of RPE65, the rate of regeneration is a linear function of the quantity of RPE65 (Figure 4A, inset), and so from their data, it is

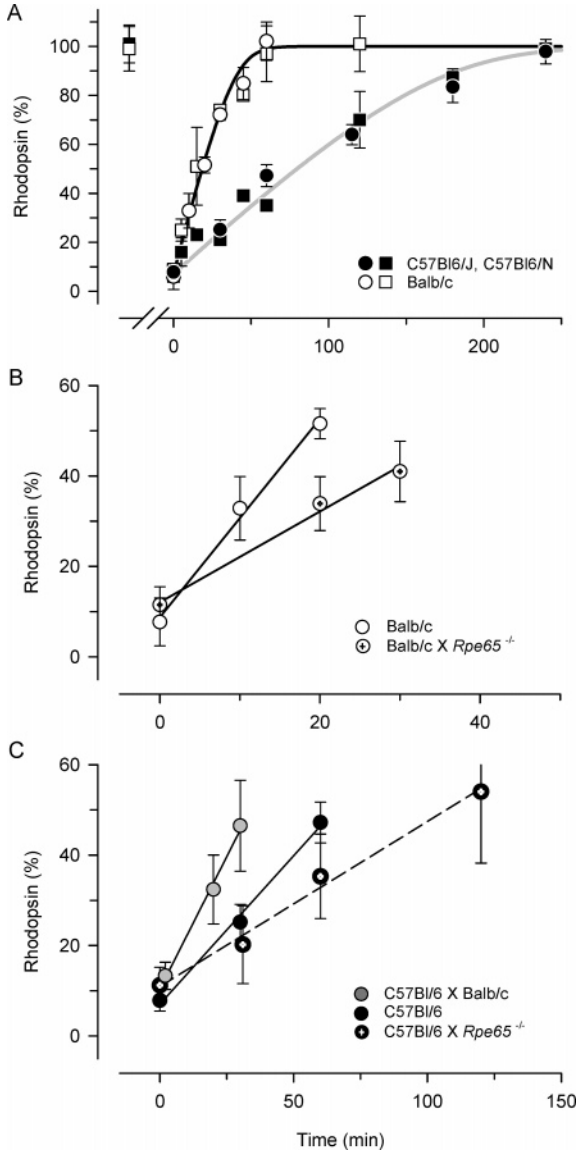

FIGURE 3: (A) Time course of rhodopsin regeneration after a nearly complete bleach in unanesthetized BALB/c and C57BL/6 mice. Data plotted as circles are from this study; data plotted as squares are from ref *19*. The smooth curves plot solutions to the rate-limited regeneration model of ref *2*, fitted by eye to each set of data: the parameters are initial bleach level $B_0 = 93\%$ (both curves), $K_m = 0.2$ (both curves), and initial regeneration rates $\nu = 2.4\%$ min^{-1} (Balb/c) and 0.58% min^{-1} (C57BL/6). (The Balb/c mice, which are albinos, were illuminated at $\sim^1/_3$ the level of the pigmented mice to produce the same initial bleach level; cf. Methods.) (B) Initial phase of rhodopsin regeneration in Balb/c (○) and Balb/c × *Rpe65*$^{-/-}$ (⊙) mice; least-squares regression lines fitted to the data have slopes of 2.2% min^{-1} (Balb/c) and 1.0% min^{-1} (Balb/c × *Rpe65*$^{-/-}$). (C) Initial phase of rhodopsin regeneration in Balb/c × C57BL/6 (gray circles), C57BL/6 (●), and C57BL/6 × *Rpe65*$^{-/-}$ (black circles with white crosses) mice; the regression lines fitted to the data have slopes of 1.2, 0.66, and 0.36% min^{-1}, respectively. Error bars are standard deviations, determined from replication with two to eight mice for each plotted point. The white circles in panel B and black circles in panel C replot data at early times from Balb/c and C57BL/6 mice in panel A. The values of 2.2 and 0.66% min^{-1} derived from the least-squares analysis of panels B and C were adopted as the final estimates of the initial rates for Balb/c and C57BL/6 mice, respectively, so that the rates for all five lines of mice were extracted by the same method.

possible to estimate the rate of production of 11-*cis*-retinal per molecule of RPE65 (Figure 4B). To effect this estimation, the rates of regeneration are first expressed in units of

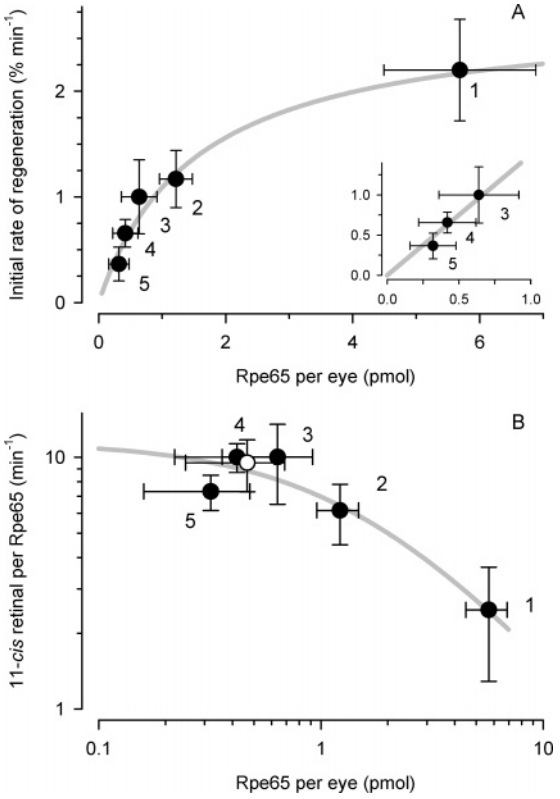

FIGURE 4: Relation between the mole quantity of RPE65 protein and the initial rate of rhodopsin regeneration in unanesthetized mice. (A) Filled symbols give the initial rate of regeneration as a function of the amount of RPE65 for each of the five murine lines investigated; numbers near points identify the strains, as follows: (1) Balb/c, (2) Balb/c × C57BL/6, (3) Balb/c × *Rpe65*$^{-/-}$, (4) C57BL/6N, and (5) C57BL/6N × *Rpe65*$^{-/-}$. The smooth curve plots the saturation relation of eq 2 with a ν_{max} of 2.75% min^{-1} and a k_m of 1.52 pmol. The inset shows the lowermost three data points, fitted with a straight line passing through the origin, and having a slope of 1.6% min^{-1} (pmol of RPE65)$^{-1}$ ($\sim\nu_{max}/k_m$), serving to confirm the linear dependence. The error bars for the abscissa values of the points come from the errors associated with determination of RPE65 (cf. Table 1), while the error bars for the ordinate values are those associated with the slope estimates obtained from fitting linear regressions to the initial phase of rhodopsin regeneration (Figure 3B,C). (B) The data from panel A have been replotted, with the ordinate values now divided by the RPE65 mole quantities, and multiplied by the total mole quantity of rhodopsin in the dark-adapted eye. The empty symbol plots the weighted average of the lowermost three points. Both this mean value and the asymptote of the theory trace yield an estimate of ~10 molecules of 11-*cis*-retinal generated per RPE65 molecule during the initial, linear phase of rhodopsin regeneration in the low-level expressors. The smooth curve represents the curve of panel A, transformed in the same manner in which the data points were; thus, ν/RPE65 (see eq 2) has been plotted.

picomoles of rhodopsin regenerated per minute; thus, the rate in fraction rhodopsin per minute is multiplied by the average quantity of rhodopsin in the dark-adapted eye, 640 pmol (Table 1). The rate so expressed is then divided by the quantity of RPE65 per eye; thus, it is found that during the linear phase of rhodopsin regeneration in these lines of mice, 11-*cis*-retinal is produced at a rate of ~10 molecules/min per molecule of RPE65 (Figure 4B).

DISCUSSION

Masking Is a Potentially Serious Artifact in Quantitative Immunoblotting. By admixing protein extract from the eyes

of *Rpe65*$^{-/-}$ mice with rRPE65, we uncovered a "masking" artifact that reduces the magnitudes of the immunoblot signals from RPE65 by 50−90% (Figure 1). In quantifying RPE65, we controlled for this problem in two ways: (1) by admixing with rRPE65 extract from eyes of *Rpe65*$^{-/-}$ mice to load SDS gels with approximately the same total protein in the absolute quantification of RPE65 in Balb/c eyes and (2) by developing a ratiometric approach to determining the amount of RPE65 in the eyes from other lines of mice relative to that in Balb/c eyes. In this investigation, we were fortunate to have an appropriate control protein extract from the eyes of *Rpe65*$^{-/-}$ mice, but in many investigations, tissue from a mouse with the target protein deleted may be either unavailable or compromised (for example, by alterations in tissue development). This result sounds a cautionary note for any investigation employing immunoblotting in quantifying proteins.

Rhodopsin Regeneration Is Rate-Limited by RPE65 in Low-Level Expressors. The initial phase of rhodopsin regeneration is rate-limited, so initially after a large bleaching exposure regeneration proceeds linearly with time (Figure 3). Though only recently recognized as such, this rate-limited behavior appears to be a universal feature of both rod and cone pigment regeneration in mammals (*2*, *24*). The mechanism underlying the rate limit is of considerable interest, because of the variation in the limit across species, because a number of disease conditions affect the rate, and because the time course of human dark adaptation is governed by the same rate-limited process, leading to the clinically useful conclusion that noninvasive dark adaptometry can be used to quantitatively assess critical features of the retinoid cycle (*2*).

Our study advances the understanding of the mechanism underlying the rate limit by establishing that the quantity of RPE65 determines the limit in the three mouse lines expressing the smallest amount of RPE65 (<1 pmol/eye). As the rate of regeneration in the mice with the highest level of RPE65 expression (Balb/c, 5.7 pmol/eye) falls more than 4-fold below the direct proportionality to RPE65 that holds in the low-level expressors (Figure 4A, inset; Figure 4B), the results also suggest that some factor other than RPE65 limits the rate of synthesis and/or delivery of 11-*cis*-retinal in Balb/c mice. To facilitate further discussion of the implications of our results for understanding the role of RPE65, we present a simplified scheme for the portion of the visual retinoid cycle that takes place in RPE cells (Scheme 1). In the discussion that follows, we will assume that rhodopsin regeneration in mice closely tracks 11-*cis*-retinal synthesis, and thus that the former can be used as a surrogate for investigating the latter in vivo. (Evidence for this assumption is reviewed in ref *2*.)

A Benchmark for the Isomerohydrolase Specific Activity. RPE65 is now well established as being necessary for isomerohydrolase activity in mice (*13*, *14*). Two hypotheses about this requirement are extant: (1) that RPE65 is required for delivery to the isomerohydrolase of its obligatory substrate, all-*trans*-retinyl ester (*5*, *15*, *16*), and (2) that RPE65 is itself the isomerohydrolase (*18*). Our observations are consistent with and have implications for both hypotheses. Thus, one would expect that in any system in which a specific substrate must be delivered to an enzyme by a carrier that at some level the carrier concentration would become rate-limiting for the enzyme activity, and the RPE65−retinyl ester substrate−carrier complex plays the same functional role as the specific substrate of any enzyme (*25*). Moreover, in the context of the hypothesis that all-*trans*-retinal ester must be delivered from a separate retinyl ester storage particle (*REST* in Scheme 1) to isomerohydrolase in the smooth endoplasmic reticulum (SER in Scheme 1) by RPE65 (*16*, *26*), our results imply that a single RPE65 molecule can shuttle back and forth from the storage 10 times per minute, presumably undergoing palmitoylation and depalmitoylation each time retinyl ester is delivered (*27*). This inference is equally valid if mRPE65 with all-*trans*-retinyl ester bound is itself a component of an isomerohydrolase complex in the smooth endoplasmic reticulum (Scheme 1). Indeed, if isomerohydrolase activity results from an obligatory complex involving mRPE65, then 10 min^{-1} sets a lower bound for the k_{cat} of the enzyme, and a benchmark for the ultimate reconstitution that will confirm its identity.

A k_{cat} of 10 min^{-1} might seem to be sufficiently low to reject the hypothesis that mRPE65 could be a component of an isomerohydrolase complex (*18*). However, the dissociation constant K_D of mRPE65 for all-*trans*-retinyl palmitate is 47 nM (*27*). If the K_D is taken as an estimate of the K_m, then the k_{cat}/K_m of such an isomerohydrolase complex would be greater than (10/60) s^{-1}/(47 × 10^{-9} M) = 4 × 10^6 M^{-1} s^{-1}, qualifying the hypothetical complex as one of high overall efficiency, and within a factor of 10 of that of catalase, whose activity is considered to approach diffusion-limited control (*25*).

Can the General Phenomenon of Rate-Limited Regeneration Be Reconciled with Specific Cases in which RPE65 Sets the Limit? Rate-limited regeneration kinetics are characteristic of all species that have been characterized, including normal humans (ν = 9% min^{-1}) and humans with greatly slowed regeneration that can be attributed to mutations in CRALBP and 11-*cis*-RDH (*2*), so it is clear that such kinetics are not restricted to individuals with low levels of RPE65. Can the generality of rate-limited regeneration kinetics be reconciled with the specific cases presented here in which the quantity of RPE65 determines the limit (Figure 4) and with deficiencies in which other retinoid processing genes determine the limit (*2*)? One hypothesis that can provide a unified explanation of all rate-limited regeneration data is one in which RPE cells contain a highly effective feedback loop that serves to stabilize the concentration of 11-*cis*-retinal. A possible mechanism of such stabilization, involving the palmitoylation-dependent switch of RPE65 from the soluble (sRPE65) to the membrane-attached (mRPE65) form, has been proposed (*27*). Retinas with different complements of the critical proteins in the stabilization loop, including RPE65, isomerohydrolase, 11-*cis*-RDH, and CRALBP (Scheme 1), would have different stable concentrations (C) of 11-*cis*-retinal. When the hypothesis of 11-*cis*-retinal stabilization is combined with the model of regeneration developed in ref *2*, the general result of rate-limited behavior with different rates follows, because the maximum rate of regeneration is predicted to be directly proportional to C (*2*).

Differential Post-Transcriptional Regulation of Leu450/Met450 RPE65 Variants Is Not the Major Cause of Variation in the Amount of RPE65 in Mice. An important question that arises from our results is what underlies the 13-fold difference between the C57BL/6 and Balb/c strains in the level of

Scheme 1: Visual Retinoid Cycle and RPE65 Cycle in Retinal Pigment Epithelium Cells[a]

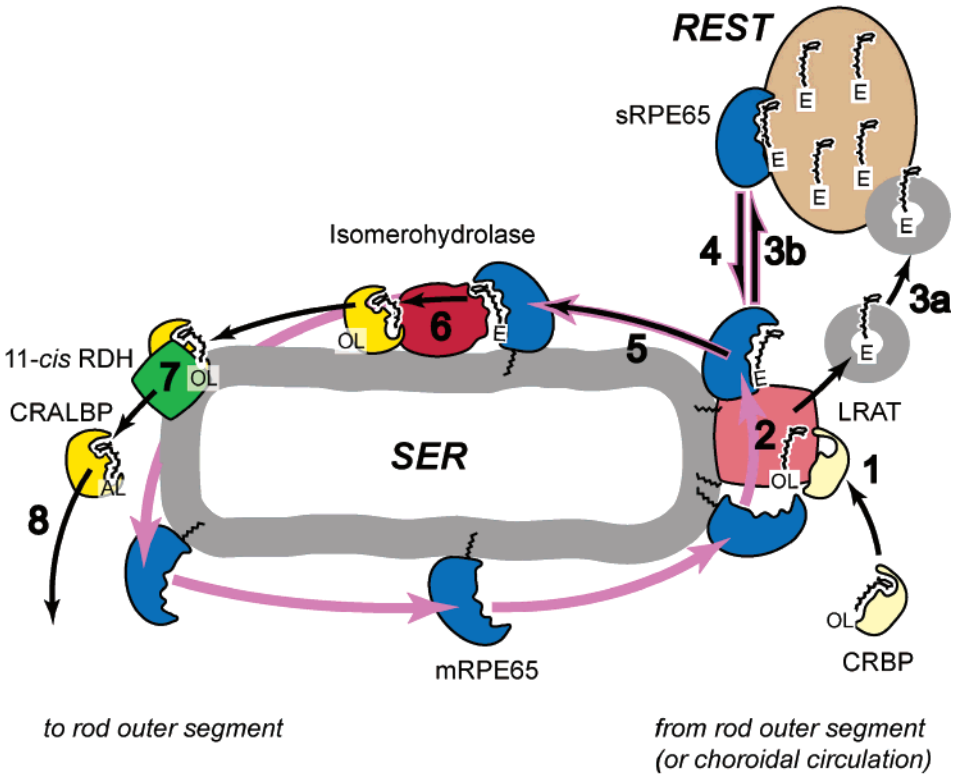

[a] Black arrows show the flow of retinoids, which enter the RPE cell as all-*trans*-retinol (vitamin A) released from the rod outer segments after rhodopsin bleaching or from the choroidal circulation (*30*), and which exit as 11-*cis*-retinal, the visual chromophore. Purple arrows illustrate the cycling of RPE65. (Where the two cycles correspond, the black arrows have been superimposed on the purple arrows.) Three chemically distinct forms of retinoid are identified: alcohol (OL tag at its terminus), aldehyde (AL), and ester (E). In step 1, all-*trans*-retinol enters the cycle chaperoned by cellular retinol binding protein (CRBP), which delivers it to lecithin retinol acyl transferase (LRAT). In step 2, LRAT converts the retinoid to the ester form, using as the acyl donor either palmitate from the membrane or a palmitoyl group attached to RPE65 (mRPE65) (*27*). In step 3, the retinyl ester is transported to the retinyl ester storage particle or *REST* (*31*) either in vesicles (3a) or by soluble, depalmitoylated, soluble RPE65 (sRPE65) (3b). In step 4, sRPE65 binds and delivers the ester from storage back to LRAT; sRPE65 is then itself palmitoylated to form the membrane-attached form mRPE65 and in step 5 delivers the esterified retinoid to the isomerohydrolase complex (*16*, *26*). In step 6, the all-*trans*-retinoid is isomerized and the ester cleaved, forming 11-*cis*-retinol, which is bound by cellular retinal binding protein (CRALBP). In step 7, 11-*cis*-retinol dehydrogenase (11-*cis*-RDH) oxidizes the *cis*-retinoid to the aldehyde form, and in step 8, the 11-*cis*-retinal is bound again by the chaperone CRALPB for delivery to opsin in the photoreceptor cells. RPE65 itself is also cycled, being transformed (step 2) from a membrane-attached form depleted of the all-*trans* ester to a soluble form [which may deliver the ester to storage or simply retrieve it (steps 3b and 4)], to the membrane-attached form loaded with the ester substrate for the isomerohydrolase (step 4). After the isomerase reaction, the RPE65 cycle and the visual retinoid cycle diverge, as the protein is recycled. Evidence presented in Figure 5 suggests that on average an RPE65 can complete its cycle ~10 times per minute.

expression of RPE65 protein (Table 1). One constraint on the answer is that message levels per allele differ by only 25% (Table 1); a previous investigation reported little variation in message levels between C57BL/6 and Balb/c strains, with substantially lower RPE65 protein levels in C57BL/6 mice, which have the Met450 variant (*19*). These observations suggest the hypothesis that the Met450 variant of RPE65 has a lower rate of expression per unit message, or lower stability than the Leu450 variant. Our observations are inconsistent with this hypothesis as the sole explanation of the difference in RPE65 expression levels in the two strains. In particular, we found that the protein-to-message ratio was much lower in Balb/c × *Rpe65*$^{-/-}$ (Leu/−) mice (PMR = 0.18) than in Balb/c (Leu/Leu) mice (PMR = 1.0) (Table 1; $t_{1df} = 9.1$, $p < 0.05$). A plausible hypothesis is that there is another factor in C57BL/6 mice that lowers the steady-state level of RPE65 protein: the crossbreeding of Balb/c with *Rpe65*$^{-/-}$ mice having a predominant C57BL/6 background (*13*) could cause transmission of the gene for this factor into the F1 cross. Indeed, in the five lines of mice examined, the PMR appears to be lower the more completely the animals have C57BL/6 background, suggesting the hypothetical factor is a dominant trait. Whatever ultimately explains the variation in RPE65 expression between strains of mice, we emphasize that our results are in no way in conflict with the hypothesis that the *amount* of RPE65 is inversely related to light-damage susceptibility (*19*, *28*), presumably because a lower level of rhodopsin regeneration slows the net production of one or more toxic retinoid byproducts produced by bleaching (*19*, *28*, *29*).

SUPPORTING INFORMATION AVAILABLE

Procedure by which absolute quantification of the amount of RPE65 in extracts of Balb/c eyes was achieved with immunoblotting. This material is available free of charge via the Internet at http://pubs.acs.org.

REFERENCES

1. McBee, J. K., Palczewski, K., Baehr, W., and Pepperberg, D. R. (2001) Confronting complexity: The interlink of phototransduction and retinoid metabolism in the vertebrate retina, *Prog. Retinal Eye Res. 20*, 469−529.

2. Lamb, T. D., and Pugh, E. N., Jr. (2004) Dark adaptation and the retinoid cycle of vision, *Prog. Retinal Eye Res. 23*, 307−380.
3. Bernstein, P. S., Law, W. C., and Rando, R. R. (1987) Biochemical characterization of the retinoid isomerase system of the eye, *J. Biol. Chem. 262*, 16848−16857.
4. Gollapalli, D. R., and Rando, R. R. (2003) All-trans-retinyl esters are the substrates for isomerization in the vertebrate visual cycle, *Biochemistry 42*, 5809−5818.
5. Moiseyev, G., Crouch, R. K., Goletz, P., Oatis, J., Jr., Redmond, T. M., and Ma, J. X. (2003) Retinyl esters are the substrate for isomerohydrolase, *Biochemistry 42* (7), 2229−2238.
6. Gollapalli, D. R., and Rando, R. R. (2003) Specific inactivation of isomerohydrolase activity by 11-cis-retinoids, *Biochim. Biophys. Acta 1651*, 93−101.
7. Simon, A., Romert, A., Gustafson, A. L., McCaffery, J. M., and Eriksson, U. (1999) Intracellular localization and membrane topology of 11-cis retinol dehydrogenase in the retinal pigment epithelium suggest a compartmentalized synthesis of 11-cis retinaldehyde, *J. Cell Sci. 112* (Part 4), 549−558.
8. Hamel, C. P., Tsilou, E., Pfeffer, B. A., Hooks, J. J., Detrick, B., and Redmond, T. M. (1993) Molecular cloning and expression of RPE65, a novel retinal pigment epithelium-specific microsomal protein that is post-transcriptionally regulated in vitro, *J. Biol. Chem. 268* (21), 15751−15757.
9. Nicoletti, A., Wong, D. J., Kawase, K., Gibson, L. H., Yang-Feng, T. L., Richards, J. E., and Thompson, D. A. (1995) Molecular characterization of the human gene encoding an abundant 61 kDa protein specific to the retinal pigment epithelium, *Hum. Mol. Genet. 4* (4), 641−649.
10. Thompson, D. A., Gyurus, P., Fleischer, L. L., Bingham, E. L., McHenry, C. L., Apfelstedt-Sylla, E., Zrenner, E., Lorenz, B., Richards, J. E., Jacobson, S. G., Sieving, P. A., and Gal, A. (2000) Genetics and phenotypes of RPE65 mutations in inherited retinal degeneration, *Invest. Ophthalmol. Visual Sci. 41* (13), 4293−4299.
11. Marlhens, F., Bareil, C., Griffoin, J. M., Zrenner, E., Amalric, P., Eliaou, C., Liu, S. Y., Harris, E., Redmond, T. M., Arnaud, B., Claustres, M., and Hamel, C. P. (1997) Mutations in RPE65 cause Leber's congenital amaurosis, *Nat. Genet. 17* (2), 139−141.
12. Gu, S. M., Thompson, D. A., Srikumari, C. R., Lorenz, B., Finckh, U., Nicoletti, A., Murthy, K. R., Rathmann, M., Kumaramanickavel, G., Denton, M. J., and Gal, A. (1997) Mutations in RPE65 cause autosomal recessive childhood-onset severe retinal dystrophy, *Nat. Genet. 17* (2), 194−197.
13. Redmond, T. M., Yu, S., Lee, E., Bok, D., Hamasaki, D., Chen, N., Goletz, P., Ma, J. X., Crouch, R. K., and Pfeifer, K. (1998) Rpe65 is necessary for production of 11-cis-vitamin A in the retinal visual cycle, *Nat. Genet. 20*, 344−351.
14. Fan, J., Rohrer, B., Moiseyev, G., Ma, J. X., and Crouch, R. K. (2003) Isorhodopsin rather than rhodopsin mediates rod function in RPE65 knock-out mice, *Proc. Natl. Acad. Sci. U.S.A. 100* (23), 13662−13667.
15. Gollapalli, D. R., Maiti, P., and Rando, R. R. (2003) RPE65 operates in the vertebrate visual cycle by stereospecifically binding all-trans-retinyl esters, *Biochemistry 42*, 11824−11830.
16. Mata, N. L., Moghrabi, W. N., Lee, J. S., Bui, T. V., Radu, R. A., Horwitz, J., and Travis, G. H. (2004) Rpe65 is a retinyl ester binding protein that presents insoluble substrate to the isomerase in retinal pigment epithelial cells, *J. Biol. Chem. 279* (1), 635−643.
17. Batten, M. L., Imanishi, Y., Maeda, T., Tu, D. C., Moise, A. R., Bronson, D., Possin, D., Van Gelder, R. N., Baehr, W., and Palczewski, K. (2004) Lecithin-retinol acyltransferase is essential for accumulation of all-trans-retinyl esters in the eye and in the liver, *J. Biol. Chem. 279*, 10422−10432.
18. Ma, J.-X., Chen, Y., Takahashi, Y., and Moiseyev, G. (2005) RPE65 is the isomerohydrolase in the retinoid visual cycle, *Invest. Ophthalmol. Visual Sci. 46* (in press).
19. Wenzel, A., Reme, C. E., Williams, T. P., Hafezi, F., and Grimm, C. (2001) The Rpe65 Leu450Met variation increases retinal resistance against light-induced degeneration by slowing rhodopsin regeneration, *J. Neurosci. 21* (1), 53−58.
20. Lyubarsky, A. L., Daniele, L. L., and Pugh, E. N., Jr. (2004) From candelas to photoisomerizations in the mouse eye by rhodopsin bleaching in situ and the light-rearing dependence of the major components of the mouse ERG, *Vision Res. 44*, 3235−3251.
21. Saari, J. C., Nawrot, M., Kennedy, B. N., Garwin, G. G., Hurley, J. B., Huang, J., Possin, D. E., and Crabb, J. W. (2001) Visual cycle impairment in cellular retinaldehyde binding protein (CRALBP) knockout mice results in delayed dark adaptation, *Neuron 29*, 739−748.
22. Redmond, T. M., and Hamel, C. P. (2000) Genetic analysis of RPE65: From human disease to mouse model, *Methods Enzymol. 316*, 705−724.
23. Nicoletti, A., Kawase, K., and Thompson, D. A. (1998) Promoter analysis of RPE65, the gene encoding a 61-kDa retinal pigment epithelium-specific protein, *Invest. Ophthalmol. Visual Sci. 39* (3), 637−644.
24. Mahroo, O. A., and Lamb, T. D. (2004) Recovery of the human photopic electroretinogram after bleaching exposures: Estimation of pigment regeneration kinetics, *J. Physiol. 554*, 417−437.
25. Fersht, A. (1977) *Enzyme Structure and Mechanism*, W. H. Freeman, New York.
26. Gollapalli, D. R., and Rando, R. R. (2003) Molecular logic of 11-cis-retinoid biosynthesis in a cone-dominated species, *Biochemistry 42*, 14921−14929.
27. Xue, L., Gollapalli, D. R., Maiti, P., Jahng, W. J., and Rando, R. R. (2004) A palmitoylation switch mechanism in the regulation of the visual cycle, *Cell 117* (6), 761−771.
28. Grimm, C., Wenzel, A., Hafezi, F., Yu, S., Redmond, T. M., and Reme, C. E. (2000) Protection of Rpe65-deficient mice identifies rhodopsin as a mediator of light-induced retinal degeneration, *Nat. Genet. 25* (1), 63−66.
29. Keller, C., Grimm, C., Wenzel, A., Hafezi, F., and Reme, C. (2001) Protective effect of halothane anesthesia on retinal light damage: Inhibition of metabolic rhodopsin regeneration, *Invest. Ophthalmol. Visual Sci. 42* (2), 476−480.
30. Qtaishat, N. M., Redmond, T. M., and Pepperberg, D. R. (2003) Acute radiolabeling of retinoids in eye tissues of normal and rpe65-deficient mice, *Invest. Ophthalmol. Visual Sci. 44* (4), 1435−1446.
31. Imanishi, Y., Batten, M. L., Piston, D. W., Baehr, W., and Palczewski, K. (2004) Noninvasive two-photon imaging reveals retinyl ester storage structures in the eye, *J. Cell Biol. 164* (3), 373−383.

BI0505363